



HAL
open science

The T -coercivity approach for solving Stokes problem: stabilization of finite element pairs

Patrick Ciarlet, Erell Jamelot

► **To cite this version:**

Patrick Ciarlet, Erell Jamelot. The T -coercivity approach for solving Stokes problem: stabilization of finite element pairs. 2024. hal-04414789

HAL Id: hal-04414789

<https://inria.hal.science/hal-04414789>

Preprint submitted on 24 Jan 2024

HAL is a multi-disciplinary open access archive for the deposit and dissemination of scientific research documents, whether they are published or not. The documents may come from teaching and research institutions in France or abroad, or from public or private research centers.

L'archive ouverte pluridisciplinaire **HAL**, est destinée au dépôt et à la diffusion de documents scientifiques de niveau recherche, publiés ou non, émanant des établissements d'enseignement et de recherche français ou étrangers, des laboratoires publics ou privés.



Distributed under a Creative Commons Attribution - NonCommercial - NoDerivatives 4.0
International License

THE T -COERCIVITY APPROACH FOR SOLVING STOKES PROBLEM: STABILIZATION OF FINITE ELEMENT PAIRS

P. CIARLET JR

*POEMS, CNRS, INRIA, ENSTA Paris, Institut Polytechnique de Paris, 91120
Palaiseau, France*

E. JAMELOT

*Université Paris-Saclay, CEA, Service de Thermo-hydraulique et de Mécanique
des Fluides, 91191 Gif-sur-Yvette cedex, France*

ABSTRACT. Using the T -coercivity theory as advocated in [1], we propose a new variational formulation of Stokes problem. With this new formulation, unstable finite element pairs can be stabilized. In addition, the numerical scheme is easy to implement, and a better approximation of the velocity and the pressure is observed numerically, especially when the viscosity is small.

Keywords. Stokes problem, T -coercivity, pressure robust variational formulation.

2020 Mathematics Subject Classification. 65N30, 35J57, 76D07

Funding. CEA SIMU/SITHY project

1. INTRODUCTION

The Stokes problem describes the steady state of incompressible Newtonian flows. They are derived from the Navier–Stokes equations [2]. With regard to numerical analysis, the study of Stokes problem helps to build an appropriate approximation of the Navier–Stokes equations. We propose here to write a new variational formulation of Stokes problem using the T -coercivity theory, following §2.3.2 in [1]. In Section 2, we recall the T -coercivity theory as written in [3]. In Section 3 we apply it to the continuous Stokes Problem. We exhibit an operator T such that the global variational formulation of Stokes Problem is T -coercive. In Section 4, we build and analyse a new variational formulation that uses explicitly this operator T . Then, in Section 5, we introduce discretizations of the new variational formulation, and we study the convergence of the discrete solution to the exact one. As a particular case, convergence is obtained for the unstable finite element pair $\mathbf{P}^1 \times P^0$. Finally, we provide some numerical experiments in Section 6 to illustrate our points and give some concluding remarks in Section 7.

E-mail addresses: `patrick.ciarlet@ensta-paris.fr`, `erell.jamelot@cea.fr`.

Date: January 22, 2024.

2. T -COERCIVITY

We recall here the T -coercivity theory as written in [3]. Consider first the variational problem, where V and W are two Hilbert spaces and $f \in V'$:

$$(2.1) \quad \text{Find } u \in V \text{ such that } \forall v \in W, a(u, v) = \langle f, v \rangle_V.$$

Classically, we know that Problem (2.1) is well-posed if $a(\cdot, \cdot)$ satisfies the stability and the solvability conditions of the so-called Banach–Nečas–Babuška (BNB) Theorem (see a.e. [4, Thm. 25.9]). For some models, one can also prove the well-posedness using the T -coercivity theory. We refer to [3] for Helmholtz-like problems, see [5], [6] and [7] for the neutron diffusion equation, and to [8] for the magnetostatic problem.

Definition 1. *Let V and W be two Hilbert spaces and $a(\cdot, \cdot)$ be a continuous and bilinear form over $V \times W$. It is T -coercive if*

$$(2.2) \quad \exists T \in \mathcal{L}(V, W), \text{ bijective, } \exists \alpha > 0, \forall v \in V, |a(v, Tv)| \geq \alpha \|v\|_V^2.$$

It is proved in [3, 1] that the T -coercivity condition is equivalent to the stability and solvability conditions of the BNB Theorem. Whereas the BNB theorem relies on an abstract inf–sup condition, T -coercivity uses explicit inf–sup operators, both at the continuous and discrete levels.

Theorem 1. *(well-posedness) Let $a(\cdot, \cdot)$ be a continuous and bilinear form. Suppose that the form $a(\cdot, \cdot)$ is T -coercive. Then Problem (2.1) is well-posed.*

3. STOKES PROBLEM

Let Ω be a connected bounded domain of \mathbb{R}^d , $d = 2, 3$, with a polygonal ($d = 2$) or Lipschitz polyhedral ($d = 3$) boundary $\partial\Omega$. We consider Stokes problem:

$$(3.1) \quad \text{Find } (\mathbf{u}, p) \text{ such that } \begin{cases} -\nu \Delta \mathbf{u} + \mathbf{grad} p = \mathbf{f}, \\ \operatorname{div} \mathbf{u} = 0. \end{cases}$$

with Dirichlet boundary conditions for the velocity \mathbf{u} and a normalization condition for the pressure p :

$$\mathbf{u} = 0 \text{ on } \partial\Omega, \quad \int_{\Omega} p = 0.$$

The vector field \mathbf{u} represents the velocity of the fluid and the scalar field p represents its pressure divided by the fluid density which is supposed to be constant. The first equation of (3.1) corresponds to the momentum balance equation and the second one corresponds to the conservation of the mass. The constant parameter $\nu > 0$ is the kinematic viscosity of the fluid. The vector field $\mathbf{f} \in \mathbf{H}^{-1}(\Omega)$ represents a body forces divided by the fluid density.

Before stating the variational formulation of Problem (3.1), we provide some definition and reminders. Let us set $\mathbf{L}^2(\Omega) = (L^2(\Omega))^d$, $\mathbf{H}_0^1(\Omega) = (H_0^1(\Omega))^d$, $\mathbf{H}^{-1}(\Omega) = (H^{-1}(\Omega))^d$ its dual space and $L_{zmv}^2(\Omega) = \{q \in L^2(\Omega) \mid \int_{\Omega} q = 0\}$. We recall that $\mathbf{H}(\operatorname{div}; \Omega) = \{\mathbf{v} \in \mathbf{L}^2(\Omega) \mid \operatorname{div} \mathbf{v} \in L^2(\Omega)\}$. Let us first recall Poincaré–Steklov inequality:

$$(3.2) \quad \exists C_{PS} > 0 \mid \forall v \in H_0^1(\Omega), \quad \|v\|_{L^2(\Omega)} \leq C_{PS} \|\mathbf{grad} v\|_{\mathbf{L}^2(\Omega)}.$$

Thanks to this result, in $H_0^1(\Omega)$, the semi-norm is equivalent to the natural norm, so that the scalar product reads $(v, w)_{H_0^1(\Omega)} = (\mathbf{grad} v, \mathbf{grad} w)_{\mathbf{L}^2(\Omega)}$ and the norm is $\|v\|_{H_0^1(\Omega)} = \|\mathbf{grad} v\|_{\mathbf{L}^2(\Omega)}$. Let $\mathbf{v}, \mathbf{w} \in \mathbf{H}_0^1(\Omega)$. We denote by $(v_i)_{i=1}^d$ (resp.

$(w_i)_{i=1}^d$) the components of \mathbf{v} (resp. \mathbf{w}), and we set $\mathbf{Grad} \mathbf{v} = (\partial_j v_i)_{i,j=1}^d \in \mathbb{L}^2(\Omega)$, where $\mathbb{L}^2(\Omega) = [L^2(\Omega)]^{d \times d}$. We have:

$$(\mathbf{Grad} \mathbf{v}, \mathbf{Grad} \mathbf{w})_{\mathbb{L}^2(\Omega)} = (\mathbf{v}, \mathbf{w})_{\mathbf{H}_0^1(\Omega)} = \sum_{i=1}^d (v_i, w_i)_{H_0^1(\Omega)}$$

and:

$$\|\mathbf{v}\|_{\mathbf{H}_0^1(\Omega)} = \left(\sum_{j=1}^d \|v_j\|_{H_0^1(\Omega)}^2 \right)^{1/2} = \|\mathbf{Grad} \mathbf{v}\|_{\mathbb{L}^2(\Omega)}.$$

Let us set $\mathbf{V} = \{\mathbf{v} \in \mathbf{H}_0^1(\Omega) \mid \operatorname{div} \mathbf{v} = 0\}$. The vector space \mathbf{V} is a closed subset of $\mathbf{H}_0^1(\Omega)$. We denote by \mathbf{V}^\perp the orthogonal of \mathbf{V} in $\mathbf{H}_0^1(\Omega)$. We recall that [2, cor. I.2.4]:

Proposition 1. *The operator $\operatorname{div} : \mathbf{H}_0^1(\Omega) \rightarrow L^2(\Omega)$ is an isomorphism of \mathbf{V}^\perp onto $L_{zmv}^2(\Omega)$. We call $C_{\operatorname{div}} \geq 1$ the constant such that:*

$$(3.3) \quad \forall p \in L_{zmv}^2(\Omega), \exists! \tilde{\mathbf{v}}_p \in \mathbf{V}^\perp \mid \operatorname{div} \tilde{\mathbf{v}}_p = p \text{ and } \|\tilde{\mathbf{v}}_p\|_{\mathbf{H}_0^1(\Omega)} \leq C_{\operatorname{div}} \|p\|_{L^2(\Omega)}.$$

In the above, we note that since

$$\forall \mathbf{v} \in \mathbf{H}_0^1(\Omega), \quad \|\mathbf{v}\|_{\mathbf{H}_0^1(\Omega)}^2 = \|\operatorname{curl} \mathbf{v}\|_{\mathbb{L}^2(\Omega)}^2 + \|\operatorname{div} \mathbf{v}\|_{L^2(\Omega)}^2,$$

one has necessarily $C_{\operatorname{div}} \geq 1$.

The variational formulation of Problem (3.1) reads:

Find $(\mathbf{u}, p) \in \mathbf{H}_0^1(\Omega) \times L_{zmv}^2(\Omega)$ such that

$$(3.4) \quad \begin{cases} \nu(\mathbf{u}, \mathbf{v})_{\mathbf{H}_0^1(\Omega)} - (p, \operatorname{div} \mathbf{v})_{L^2(\Omega)} &= \langle \mathbf{f}, \mathbf{v} \rangle_{\mathbf{H}_0^1(\Omega)} & \forall \mathbf{v} \in \mathbf{H}_0^1(\Omega); \\ (q, \operatorname{div} \mathbf{u})_{L^2(\Omega)} &= 0 & \forall q \in L_{zmv}^2(\Omega). \end{cases}$$

Classically, one proves that Problem (3.4) is well-posed using Poincaré-Steklov inequality (3.2) and Prop. 1. Check for instance the proof of [2, Thm. I.5.1].

Let us set $\mathcal{X} = \mathbf{H}_0^1(\Omega) \times L_{zmv}^2(\Omega)$ which is a Hilbert space which we endow with the following norm:

$$(3.5) \quad \|(\mathbf{v}, q)\|_{\mathcal{X}, \nu} = \left(\|\mathbf{v}\|_{\mathbf{H}_0^1(\Omega)}^2 + \nu^{-2} \|q\|_{L^2(\Omega)}^2 \right)^{1/2}.$$

We define the following bilinear symmetric and continuous form:

$$(3.6) \quad \begin{cases} a_0 : \mathcal{X} \times \mathcal{X} & \rightarrow \mathbb{R} \\ (\mathbf{u}', p') \times (\mathbf{v}, q) & \mapsto \nu(\mathbf{u}', \mathbf{v})_{\mathbf{H}_0^1(\Omega)} - (p', \operatorname{div} \mathbf{v})_{L^2(\Omega)} - (q, \operatorname{div} \mathbf{u}')_{L^2(\Omega)} \end{cases}.$$

We also define the linear and continuous form:

$$(3.7) \quad \begin{cases} \ell_0 : \mathcal{X} & \rightarrow \mathbb{R} \\ (\mathbf{v}, q) & \mapsto \langle \mathbf{f}, \mathbf{v} \rangle_{\mathbf{H}_0^1(\Omega)} \end{cases}.$$

We can write Problem (3.1) in an equivalent way as follows:

$$(3.8) \quad \text{Find } (\mathbf{u}, p) \in \mathcal{X} \text{ such that } a_0((\mathbf{u}, p), (\mathbf{v}, q)) = \ell_0((\mathbf{v}, q)) \quad \forall (\mathbf{v}, q) \in \mathcal{X}.$$

Let us prove that Problem (3.8) is well-posed using the T -coercivity theory.

Proposition 2. *The bilinear form $a_0(\cdot, \cdot)$ is T -coercive:*

$$(3.9) \quad \begin{aligned} & \exists T \in \mathcal{L}(\mathcal{X}), \text{ bijective, } \exists \alpha > 0, \forall (\mathbf{u}', p') \in \mathcal{X}, \\ & a_0((\mathbf{u}', p'), T((\mathbf{u}', p'))) \geq \alpha \|(\mathbf{u}', p')\|_{\mathcal{X}, \nu}^2. \end{aligned}$$

Proof. We follow here the proof given in [9, 10]. Let us consider $(\mathbf{u}', p') \in \mathcal{X}$ and let us build $(\mathbf{v}^*, q^*) = T(\mathbf{u}', p') \in \mathcal{X}$ satisfying (2.2) (with $V = \mathcal{X}$). We need three main steps.

1. According to Prop. 1, there exists $\tilde{\mathbf{v}}_{p'} \in \mathbf{V}^\perp$ such that:

$$(3.10) \quad \operatorname{div} \tilde{\mathbf{v}}_{p'} = p' \text{ in } \Omega \text{ and } \|\tilde{\mathbf{v}}_{p'}\|_{\mathbf{H}_0^1(\Omega)} \leq C_{\operatorname{div}} \|p'\|_{L^2(\Omega)}.$$

Let us set $(\mathbf{v}^*, q^*) := (\gamma \mathbf{u}' - \nu^{-1} \tilde{\mathbf{v}}_{p'}, -\gamma p')$, with $\gamma > 0$. We obtain:

$$(3.11) \quad a_0((\mathbf{u}', p'), (\mathbf{v}^*, q^*)) = \nu \gamma \|\mathbf{u}'\|_{\mathbf{H}_0^1(\Omega)}^2 + \nu^{-1} \|p'\|_{L^2(\Omega)}^2 - (\mathbf{u}', \tilde{\mathbf{v}}_{p'})_{\mathbf{H}_0^1(\Omega)}.$$

2. In order to bound the last term of (3.11), we use Young inequality and then inequality (3.10), so that for all $\eta > 0$:

$$(3.12) \quad (\mathbf{u}', \tilde{\mathbf{v}}_{p'})_{\mathbf{H}_0^1(\Omega)} \leq \frac{\eta}{2} \|\mathbf{u}'\|_{\mathbf{H}_0^1(\Omega)}^2 + \frac{\eta^{-1}}{2} (C_{\operatorname{div}})^2 \|p'\|_{L^2(\Omega)}^2.$$

3. Using the bound (3.12) in (3.11) and choosing $\eta = \nu \gamma$, we get:

$$a_0((\mathbf{u}', p'), (\mathbf{v}^*, q^*)) \geq \nu \left(\frac{\gamma}{2} \|\mathbf{u}'\|_{\mathbf{H}_0^1(\Omega)}^2 + \nu^{-2} \left(1 - \frac{\gamma^{-1}}{2} (C_{\operatorname{div}})^2 \right) \|p'\|_{L^2(\Omega)}^2 \right).$$

Consider now $\gamma = (C_{\operatorname{div}})^2$. We obtain:

$$a_0((\mathbf{u}', p'), (\mathbf{v}^*, q^*)) \geq \nu C_{\min} \|(\mathbf{u}', p')\|_{\mathcal{X}, \nu}^2 \text{ where } C_{\min} = \frac{1}{2} \min((C_{\operatorname{div}})^2, 1) = \frac{1}{2}.$$

We obtain (3.9) with $\alpha = \nu C_{\min}$. The operator T such that $T((\mathbf{u}', p')) = (\mathbf{v}^*, q^*)$ is linear and continuous:

$$\begin{aligned} \|T((\mathbf{u}', p'))\|_{\mathcal{X}, \nu}^2 &:= \|\mathbf{v}^*\|_{\mathbf{H}_0^1(\Omega)}^2 + \nu^{-2} \|q^*\|_{L^2(\Omega)}^2 \\ &\leq 2\gamma^2 \|\mathbf{u}'\|_{\mathbf{H}_0^1(\Omega)}^2 + 2\nu^{-2} \|\tilde{\mathbf{v}}_{p'}\|_{\mathbf{H}_0^1(\Omega)}^2 + \gamma^2 \nu^{-2} \|p'\|_{L^2(\Omega)}^2, \\ &\leq 2(C_{\operatorname{div}})^4 \|\mathbf{u}'\|_{\mathbf{H}_0^1(\Omega)}^2 + ((2(C_{\operatorname{div}})^2 + (C_{\operatorname{div}})^4) \nu^{-2} \|p'\|_{L^2(\Omega)}^2), \\ &\leq (C_{\max})^2 \|(\mathbf{u}', p')\|_{\mathcal{X}, \nu}^2, \end{aligned}$$

where $C_{\max} = C_{\operatorname{div}} \max(\sqrt{2}C_{\operatorname{div}}, (2 + (C_{\operatorname{div}})^2)^{1/2})$.

Remark that, given $(\mathbf{v}^*, q^*) \in \mathcal{X}$, choosing $(\mathbf{u}', p') = (\gamma^{-1} \mathbf{v}^* - \gamma^{-2} \nu^{-1} \tilde{\mathbf{v}}_{q^*}, -\gamma^{-1} q^*)$ yields $T((\mathbf{u}', p')) = (\mathbf{v}^*, q^*)$. Hence, the operator $T \in \mathcal{L}(\mathcal{X})$ is bijective. \square

We can now prove the

Theorem 2. *Problem (3.8) is well-posed. It admits one and only one solution such that:*

$$(3.13) \quad \forall \mathbf{f} \in \mathbf{H}^{-1}(\Omega), \quad \begin{cases} \|\mathbf{u}\|_{\mathbf{H}_0^1(\Omega)} \leq \nu^{-1} \|\mathbf{f}\|_{\mathbf{H}^{-1}(\Omega)}, \\ \|p\|_{L^2(\Omega)} \leq C_{\operatorname{div}} \|\mathbf{f}\|_{\mathbf{H}^{-1}(\Omega)}. \end{cases}$$

Proof. According to Prop. 2, the continuous bilinear form $a_0(\cdot, \cdot)$ is T -coercive. Hence, according to Theorem 1, Problem (3.8) is well-posed. Let us now derive (3.13). Consider (\mathbf{u}, p) the unique solution of Problem (3.8). Choosing $\mathbf{v} = 0$, we obtain that $\forall q \in L_{zmv}^2(\Omega)$, $(q, \operatorname{div} \mathbf{u})_{L^2(\Omega)} = 0$, so that $\mathbf{u} \in \mathbf{V}$. Now, choosing $\mathbf{v} = \mathbf{u}$ and using Cauchy-Schwarz inequality, we have: $\nu \|\mathbf{u}\|_{\mathbf{H}_0^1(\Omega)}^2 = \langle \mathbf{f}, \mathbf{u} \rangle_{\mathbf{H}_0^1(\Omega)} \leq \|\mathbf{f}\|_{\mathbf{H}^{-1}(\Omega)} \|\mathbf{u}\|_{\mathbf{H}_0^1(\Omega)}$, so that: $\|\mathbf{u}\|_{\mathbf{H}_0^1(\Omega)} \leq \nu^{-1} \|\mathbf{f}\|_{\mathbf{H}^{-1}(\Omega)}$. Next, we choose, in (3.8),

$q = 0$ and $\mathbf{v} = -\tilde{\mathbf{v}}_p \in \mathbf{V}^\perp$, where $\operatorname{div} \tilde{\mathbf{v}}_p = p$ and $\|\tilde{\mathbf{v}}_p\|_{\mathbf{H}_0^1(\Omega)} \leq C_{\operatorname{div}} \|p\|_{L^2(\Omega)}$ (see Prop. 1). Since $\mathbf{u} \in \mathbf{V}$, it holds that $(\mathbf{u}, \tilde{\mathbf{v}}_p)_{\mathbf{H}_0^1(\Omega)} = 0$. This gives:

$$\begin{aligned} \|p\|_{L^2(\Omega)}^2 &= (p, \operatorname{div} \tilde{\mathbf{v}}_p)_{L^2(\Omega)} = -\langle \mathbf{f}, \tilde{\mathbf{v}}_p \rangle_{\mathbf{H}_0^1(\Omega)}, \\ &\leq \|\mathbf{f}\|_{\mathbf{H}^{-1}(\Omega)} \|\tilde{\mathbf{v}}_p\|_{\mathbf{H}_0^1(\Omega)} \leq C_{\operatorname{div}} \nu^{-1} \|\mathbf{f}\|_{\mathbf{H}^{-1}(\Omega)} \|p\|_{L^2(\Omega)}, \end{aligned}$$

so that: $\|p\|_{L^2(\Omega)} \leq C_{\operatorname{div}} \|\mathbf{f}\|_{\mathbf{H}^{-1}(\Omega)}$. \square

4. NEW VARIATIONAL FORMULATIONS

4.1. Using T -coercivity. Let $\gamma = (C_{\operatorname{div}})^2$. In Prop. 2, we introduced the operator $T \in \mathcal{L}(\mathcal{X})$ defined by:

$$(4.1) \quad \begin{cases} T : \mathcal{X} & \rightarrow \mathbb{R} \\ (\mathbf{v}, q) & \mapsto (\gamma \mathbf{v} - \nu^{-1} \tilde{\mathbf{v}}_q, -\gamma q) \end{cases},$$

where $\tilde{\mathbf{v}}_q \in \mathbf{V}^\perp$ is given by (3.3): $\operatorname{div} \tilde{\mathbf{v}}_q = q$ and $\|\tilde{\mathbf{v}}_q\|_{\mathbf{H}_0^1(\Omega)} \leq C_{\operatorname{div}} \|q\|_{L^2(\Omega)}$. We now write the variational formulation (3.8) with test function $T((\mathbf{v}, q))$ instead of (\mathbf{v}, q) . Let us define $\tilde{a}_\gamma((\mathbf{u}', p'), (\mathbf{v}, q)) = a_0((\mathbf{u}', p'), T(\mathbf{v}, q))$. We have:

$$(4.2) \quad \begin{aligned} \tilde{a}_\gamma((\mathbf{u}', p'), (\mathbf{v}, q)) &= \nu \gamma (\mathbf{u}', \mathbf{v})_{\mathbf{H}_0^1(\Omega)} - (\mathbf{u}', \tilde{\mathbf{v}}_q)_{\mathbf{H}_0^1(\Omega)} \\ &\quad - \gamma (p', \operatorname{div} \mathbf{v})_{L^2(\Omega)} + \nu^{-1} (p', q)_{L^2(\Omega)} \\ &\quad + \gamma (q, \operatorname{div} \mathbf{u}')_{L^2(\Omega)}. \end{aligned}$$

According to Prop. 2, we have the...

Proposition 3. *The bilinear form (4.2) is coercive.*

Introducing $\ell_\gamma((\mathbf{v}, q)) := \ell_0(T(\mathbf{v}, q))$, we can propose a first new variational formulation to Problem (3.1), which reads:

$$(4.3) \quad \text{Find } (\mathbf{u}, p) \in \mathcal{X} \text{ such that } \tilde{a}_\gamma((\mathbf{u}, p), (\mathbf{v}, q)) = \ell_\gamma((\mathbf{v}, q)) \quad \forall (\mathbf{v}, q) \in \mathcal{X}.$$

Using the bijectivity of T , it is obvious that (4.3) is equivalent to (3.8), so well-posedness of (4.3) is a direct consequence of the well-posedness of (3.8), and vice versa.

Below, we provide a direct proof of why solutions to (4.3) actually solve Problem (3.1). To that aim, we need to provide an "explicit" expression of $\ell_\gamma((\mathbf{v}, q))$, which we will prove useful later on. We recall that:

$$(4.4) \quad \forall \mathbf{f}' \in \mathbf{H}^{-1}(\Omega), \quad \exists! (z_{\mathbf{f}'}, \mathbf{w}_{\mathbf{f}'}) \in L_{zmv}^2(\Omega) \times \mathbf{V}$$

$$\mathbf{f}' = \mathbf{grad} z_{\mathbf{f}'} + \mathbf{curl} \operatorname{curl} \mathbf{w}_{\mathbf{f}'},$$

where $(\mathbf{w}_{\mathbf{f}'}, z_{\mathbf{f}'})$ satisfy (3.1) $_{\nu=1}$ with data \mathbf{f}' . We have in the sense of distributions:

$$(4.5) \quad -\Delta(\cdot) = -\mathbf{curl} \operatorname{curl}(\cdot) + \mathbf{grad} \operatorname{div}(\cdot).$$

Proposition 4. *Let $\mathbf{f}' \in \mathbf{H}^{-1}(\Omega)$. Given, $q \in L_{zmv}^2$, let $\tilde{\mathbf{v}}_q \in \mathbf{V}^\perp$ be defined by (3.3). We have:*

$$(4.6) \quad \langle \mathbf{f}', \tilde{\mathbf{v}}_q \rangle_{\mathbf{H}_0^1(\Omega)} = -(z_{\mathbf{f}'}, q)_{L^2(\Omega)}.$$

Proposition 5. *The bilinear form (4.7) is coercive.*

Proof. We have:

$$\begin{aligned} a_\gamma((\mathbf{u}', p'), (\mathbf{u}', p')) &= \nu \gamma \|\mathbf{u}'\|_{\mathbf{H}_0^1(\Omega)}^2 + \nu^{-1} \|p'\|_{L^2(\Omega)}^2, \\ &\geq \nu \min(1, \gamma) \|(\mathbf{u}', p')\|_{\mathcal{X}, \nu}^2. \end{aligned}$$

□

The bilinear form $a_\gamma(\cdot, \cdot)$ being coercive for any $\gamma > 0$, we consider $a_1(\cdot, \cdot)$ to fix ideas. We now propose a second new variational formulation to Problem (3.1), which reads:

$$(4.8) \quad \begin{cases} \text{Find } (\mathbf{u}, p) \in \mathcal{X} \text{ such that} \\ a_1((\mathbf{u}, p), (\mathbf{v}, q)) = \langle \mathbf{f}, \mathbf{v} \rangle_{\mathbf{H}_0^1(\Omega)} + \nu^{-1} (z_{\mathbf{f}}, q)_{L^2(\Omega)} \quad \forall (\mathbf{v}, q) \in \mathcal{X}. \end{cases}$$

Theorem 4. *The Problem (4.8) is well-posed and is equivalent to Problem (3.1).*

Proof. The bilinear form $a_1(\cdot, \cdot)$ is continuous and coercive. Let $\mathbf{f} \in \mathbf{H}^{-1}(\Omega)$, and let $z_{\mathbf{f}}$ be given by (4.4), the linear form $\ell_1(\cdot)$ is continuous. According to Lax-Milgram Theorem, Problem (4.8) is well-posed. It exists a unique solution (\mathbf{u}, p) which depends continuously on the data.

Regarding the equivalence with Problem (3.1), we already observed that solving (4.3) is equivalent to solving (3.8), and that both of them are equivalent to solving Problem (3.1). Then, if (\mathbf{u}, p) solves Problem (3.1) with data $\mathbf{f} \in \mathbf{H}^{-1}(\Omega)$, one has in particular that $\mathbf{u} \in \mathbf{V}$. Hence it follows from the above that (\mathbf{u}, p) solves (4.8) with data \mathbf{f} , resp. $z_{\mathbf{f}}$ given by (4.4).

Conversely, assume that (\mathbf{u}, p) solves (4.8), with data $\mathbf{f} \in \mathbf{H}^{-1}(\Omega)$ and $z_{\mathbf{f}}$ given by (4.4). Denote by $(\mathbf{u}^\dagger, p^\dagger)$ the solution to Problem (3.1) with data \mathbf{f} . According to the above and by linearity, $(\mathbf{u} - \mathbf{u}^\dagger, p - p^\dagger)$ solves (4.8) with vanishing data, hence to is equal to $(\mathbf{0}, 0)$ by uniqueness: in other words, (\mathbf{u}, p) solves Problem (3.1) with data \mathbf{f} . □

Notice that we can write problem (4.8) with two equations as:

$$(4.9) \quad \begin{cases} \text{Find } (\mathbf{u}, p) \in \mathbf{H}_0^1(\Omega) \times L_{zmv}^2(\Omega) \text{ such that} \\ (i) \quad \nu (\mathbf{u}, \mathbf{v})_{\mathbf{H}_0^1(\Omega)} - (p, \operatorname{div} \mathbf{v})_{L^2(\Omega)} = \langle \mathbf{f}, \mathbf{v} \rangle_{\mathbf{H}_0^1(\Omega)} \quad \forall \mathbf{v} \in \mathbf{H}_0^1(\Omega), \\ (ii) \quad (q, \operatorname{div} \mathbf{u})_{L^2(\Omega)} + \nu^{-1} (p, q)_{L^2(\Omega)} = \nu^{-1} (z_{\mathbf{f}}, q)_{L^2(\Omega)} \quad \forall q \in L_{zmv}^2(\Omega). \end{cases}$$

This new variational formulation appears as a stabilized variational formulation, in the sense of §II.1.2 in [2], pages 120-123. It can be solved once $z_{\mathbf{f}}$, or a suitable approximation of $z_{\mathbf{f}}$, is available. This suggests to use (4.9) as a *post processing step* as follows:

- Compute $z_{\mathbf{f}}$ by solving numerically the Stokes problem (3.4) with $\nu = 1$, and data \mathbf{f} ;
- Solve (4.9) with the data \mathbf{f} and the computed $z_{\mathbf{f}}$.

Notice that we can recover that the solution \mathbf{u} to (4.9) belongs to \mathbf{V} in a simple manner: let us split $\mathbf{u} = \mathbf{u}_0 + \mathbf{u}_\perp$, where $(\mathbf{u}_0, \mathbf{u}_\perp) \in \mathbf{V} \times \mathbf{V}^\perp$, so that $\operatorname{div} \mathbf{u} = \operatorname{div} \mathbf{u}_\perp$. Choosing $\mathbf{v} = \mathbf{u}_\perp$ in (4.9)-(i), and $q = \operatorname{div} \mathbf{u}$ in (4.9)-(ii), we obtain:

$$(4.10) \quad \begin{cases} (i) \quad \nu \|\mathbf{u}_\perp\|_{\mathbf{H}_0^1(\Omega)}^2 - (p, \operatorname{div} \mathbf{u})_{L^2(\Omega)} = \langle \mathbf{f}, \mathbf{u}_\perp \rangle_{\mathbf{H}_0^1(\Omega)} = -(z_{\mathbf{f}}, \operatorname{div} \mathbf{u})_{L^2(\Omega)}, \\ (ii) \quad \|\operatorname{div} \mathbf{u}\|_{L^2(\Omega)}^2 + \nu^{-1} (p, \operatorname{div} \mathbf{u})_{L^2(\Omega)} = \nu^{-1} (z_{\mathbf{f}}, \operatorname{div} \mathbf{u})_{L^2(\Omega)}. \end{cases}$$

Summing (4.10)-(i) and (4.10)-(ii) times ν , we obtain:

$$\nu \left(\|\mathbf{u}_\perp\|_{\mathbf{H}_0^1(\Omega)}^2 + \|\operatorname{div} \mathbf{u}\|_{L^2(\Omega)}^2 \right) = 0.$$

Hence, $\mathbf{u}_\perp = 0$ and $\operatorname{div} \mathbf{u} = 0$.

4.3. Without orthogonality. Let us briefly consider what would happen if we were to consider a right inverse of the divergence operator, that is different than the one proposed in Prop. 1. For example, with values in the whole of $\mathbf{H}_0^1(\Omega)$ (not restricted to \mathbf{V}^\perp). Such an operator $q \mapsto \bar{\mathbf{v}}_q$ is considered in Section 3.1 of [11], in the case of a 2D domain with a smooth boundary. For this operator, let $\bar{C}_{\operatorname{div}}$ be a constant such that:

$$(4.11) \quad \forall q \in L^2_{zmv}(\Omega), \exists \bar{\mathbf{v}}_q \in \mathbf{H}_0^1(\Omega) \mid \operatorname{div} \bar{\mathbf{v}}_q = q \text{ and } \|\bar{\mathbf{v}}_q\|_{\mathbf{H}_0^1(\Omega)} \leq \bar{C}_{\operatorname{div}} \|q\|_{L^2(\Omega)}.$$

In general, $\bar{\mathbf{v}}_q$ does not belong to \mathbf{V}^\perp , cf. [11].

Let $\gamma = (\bar{C}_{\operatorname{div}})^2$. T -coercivity can be obtained as before, with the operator

$$(4.12) \quad \begin{cases} \bar{T} : \mathcal{X} & \rightarrow \mathbb{R} \\ (\mathbf{v}, q) & \mapsto (\gamma \mathbf{v} - \nu^{-1} \bar{\mathbf{v}}_q, -\gamma q) \end{cases},$$

Define $\bar{a}_\gamma((\mathbf{u}', p'), (\mathbf{v}, q)) = a_0((\mathbf{u}', p'), \bar{T}(\mathbf{v}, q))$. We have:

$$(4.13) \quad \begin{aligned} \bar{a}_\gamma((\mathbf{u}', p'), (\mathbf{v}, q)) &= \nu \gamma (\mathbf{u}', \mathbf{v})_{\mathbf{H}_0^1(\Omega)} - (\mathbf{u}', \bar{\mathbf{v}}_q)_{\mathbf{H}_0^1(\Omega)} \\ &\quad - \gamma (p', \operatorname{div} \mathbf{v})_{L^2(\Omega)} + \nu^{-1} (p', q)_{L^2(\Omega)} \\ &\quad + \gamma (q, \operatorname{div} \mathbf{u}')_{L^2(\Omega)}. \end{aligned}$$

However, for $\mathbf{u}' \in \mathbf{V}$ (that is for solutions (\mathbf{u}', p) to Problem (4.3)), the term $(\mathbf{u}', \bar{\mathbf{v}}_q)_{\mathbf{H}_0^1(\Omega)}$ can no longer be removed from the expression (4.2) of the bilinear form \bar{a}_γ . As a matter of fact one has

$$(\mathbf{u}', \bar{\mathbf{v}}_q)_{\mathbf{H}_0^1(\Omega)} = (\operatorname{curl} \mathbf{u}', \operatorname{curl} \bar{\mathbf{v}}_q)_{\mathbf{L}^2(\Omega)}.$$

Hence, in the non-orthogonal case, one has to choose an ad hoc constant $\gamma > 0$ to ensure T -coercivity (cf. proposition 2).

Similarly in the expression of the right-hand side $\bar{\ell}_\gamma$.

Proposition 6. *Let $\mathbf{f}' \in \mathbf{H}^{-1}(\Omega)$ be decomposed as in (4.4). Given, $q \in L^2_{zmv}(\Omega)$, let $\bar{\mathbf{v}}_q \in \mathbf{H}_0^1(\Omega)$ be defined by (4.11). We have:*

$$(4.14) \quad \langle \mathbf{f}', \bar{\mathbf{v}}_q \rangle_{\mathbf{H}_0^1(\Omega)} = -(z_{\mathbf{f}'}, q)_{L^2(\Omega)} - (\operatorname{curl} \mathbf{w}_{\mathbf{f}'}, \operatorname{curl} \bar{\mathbf{v}}_q)_{\mathbf{L}^2(\Omega)}.$$

Proof. Straightforward. \square

To conclude the non-orthogonal case, we observe that the problem, if split as in (4.9), leads to a more intricate variational formulation, which reads

$$\begin{cases} \text{Find } (\mathbf{u}, p) \in \mathbf{H}_0^1(\Omega) \times L^2_{zmv}(\Omega) \text{ such that} \\ (i)' \quad \nu (\mathbf{u}, \mathbf{v})_{\mathbf{H}_0^1(\Omega)} - (p, \operatorname{div} \mathbf{v})_{L^2(\Omega)} = \langle \mathbf{f}, \mathbf{v} \rangle_{\mathbf{H}_0^1(\Omega)} & \forall \mathbf{v} \in \mathbf{H}_0^1(\Omega), \\ (ii)' \quad -(\mathbf{u}, \bar{\mathbf{v}}_q)_{\mathbf{H}_0^1(\Omega)} + \gamma (q, \operatorname{div} \mathbf{u})_{L^2(\Omega)} + \nu^{-1} (p, q)_{L^2(\Omega)} \\ \quad = \nu^{-1} (z_{\mathbf{f}}, q)_{L^2(\Omega)} + \nu^{-1} (\operatorname{curl} \mathbf{w}_{\mathbf{f}}, \operatorname{curl} \bar{\mathbf{v}}_q)_{\mathbf{L}^2(\Omega)} & \forall q \in L^2_{zmv}(\Omega). \end{cases}$$

Regarding the right-hand side in (ii)', it requires the knowledge of both z_f and of $\mathbf{w}_{\mathbf{f}}$ (or of suitable approximations): a *two-step* procedure could be used as before (see the end of §4.2). One needs to evaluate also $(\mathbf{u}, \bar{\mathbf{v}}_q)_{\mathbf{H}_0^1(\Omega)} = (\operatorname{curl} \mathbf{u}, \operatorname{curl} \bar{\mathbf{v}}_q)_{\mathbf{L}^2(\Omega)}$ in the left-hand side of (ii'). The latter part requires some knowledge of the right

inverse of the divergence operator, and it does not seem to be achievable numerically at a reasonable cost.

5. DISCRETIZATION

5.1. A foreword on classical discretizations. To fix ideas, let us consider a discretization to solve the classical variational formulation (3.4) (conforming Taylor-Hood finite elements [12], nonconforming Crouzeix-Raviart finite elements [13], etc.). Let us call the discrete spaces $\mathbf{V}_{0,h} \subset \mathbf{H}_0^1(\Omega)$ and $Q_h \subset L_{zmv}^2(\Omega)$. Then to prove the discrete T -coercivity, we need to state the discrete counterpart to Proposition 1. To do so, we can build a family of linear operators $\Pi_c^h : \mathbf{H}_0^1(\Omega) \rightarrow \mathbf{V}_{0,h}$, known as Fortin operators, such that (see a.e. [14, §8.4.1]):

$$(5.1) \quad \exists C_c \mid \forall h, \forall \mathbf{v} \in \mathbf{H}_0^1(\Omega) \quad \|\mathbf{Grad} \Pi_c^h \mathbf{v}\|_{\mathbb{L}^2(\Omega)} \leq C_c \|\mathbf{Grad} \mathbf{v}\|_{\mathbb{L}^2(\Omega)},$$

$$(5.2) \quad \forall h, \forall \mathbf{v} \in \mathbf{H}_0^1(\Omega), \forall q_h \in Q_h \quad (\operatorname{div} \Pi_c^h \mathbf{v}, q_h)_{L^2(\Omega)} = (\operatorname{div} \mathbf{v}, q_h)_{L^2(\Omega)}.$$

In the conforming case, we rely on the bilinear form $a_0(\cdot, \cdot)$ to state the discrete variational formulation. On the other hand, using a nonconforming discretization, although we will not use the bilinear form $a_0(\cdot, \cdot)$ to exhibit the discrete variational formulation, we will need a similar operator to (5.1)-(5.2) to prove the discrete T -coercivity [15].

5.2. Discretizations. Consider $(\mathcal{T}_h)_h$ a simplicial triangulation sequence of Ω . For all $D \subset \mathbb{R}^d$, and $k \in \mathbb{N}$, we call $P^k(D)$ the set of order k polynomials on D , $\mathbf{P}^k(D) = (P^k(D))^d$, and we consider the broken polynomial space:

$$P_{disc}^k(\mathcal{T}_h) = \{q \in L^2(\Omega); \quad \forall T \in \mathcal{T}_h, q|_T \in P^k(T)\}.$$

We use the notation $P^0(\mathcal{T}_h)$ for $P_{disc}^0(\mathcal{T}_h)$.

We define the spaces of P^k -Lagrange functions:

$$\begin{aligned} V_h^k &:= \{v_h \in H^1(\Omega); \quad \forall T \in \mathcal{T}_h, v_h|_T \in P^k(T)\} \\ \mathbf{V}_{0,h}^k &:= \{v_h \in V_h^k; \quad v_h|_{\partial\Omega} = 0\}. \end{aligned}$$

We set $\mathbf{V}_h^k := (V_h^k)^d$ and $\mathbf{V}_{0,h}^k := (V_{0,h}^k)^d$. We call $Q_h^k := P_{disc}^k(\mathcal{T}_h) \cap L_{zmv}^2(\Omega)$.

Notice that $\mathbf{V}_{0,h}^k \times Q_h^{k-1} \subset \mathbf{H}_0^1(\Omega) \times L_{zmv}^2(\Omega)$ and $\operatorname{div} \mathbf{V}_{0,h}^k \subset Q_h^{k-1}$.

It is well known that discretizing (3.4) with $\mathbf{P}^k - P_{disc}^{k-1}$ finite element, $k \geq 1$, is not stable on all shape regular meshes [14]. A wide range of strategies to get round this problem have been explored for years. Below is a quick overview of these strategies:

- The discrete velocity space can be enriched see [16, 17, 18, 19, 20] for $k = 1$.
- The discrete variational formulation can be stabilized, see [21, 22, 23, 24] for $k = 1$, [25] for $k = 2$.
- The mesh can be designed in such a way that the discrete inf-sup condition applies, see [26, 27, 28] for $k > 1$.

Let $k \geq 1$. The (conforming) discretization of Problem (4.9) with $\mathbf{P}^k - P_{disc}^{k-1}$ finite element reads:

$$(5.3) \quad \left\{ \begin{array}{l} \text{Find } (\mathbf{u}_h, p_h) \in \mathbf{V}_{0,h}^k \times Q_h^{k-1} \text{ such that} \\ \nu (\mathbf{u}_h, \mathbf{v}_h)_{\mathbf{H}_0^1(\Omega)} - (p_h, \operatorname{div} \mathbf{v}_h)_{L^2(\Omega)} = \langle \mathbf{f}, \mathbf{v}_h \rangle_{\mathbf{H}_0^1(\Omega)} \quad \forall \mathbf{v}_h \in \mathbf{V}_{0,h}^k, \\ (q_h, \operatorname{div} \mathbf{u}_h)_{L^2(\Omega)} + \nu^{-1} (p_h, q_h)_{L^2(\Omega)} = \nu^{-1} (z\mathbf{f}, q_h)_{L^2(\Omega)} \quad \forall q_h \in Q_h^{k-1}. \end{array} \right.$$

Let us write $\mathbf{f} = -\nu\Delta\mathbf{u} + \mathbf{grad} z_{\mathbf{f}}$, so that Problem (5.3) reads:

$$(5.4) \quad \begin{cases} \text{Find } (\mathbf{u}_h, p_h) \in \mathbf{V}_{0,h}^k \times Q_h^{k-1} \text{ such that for all } (\mathbf{v}_h, q_h) \in \mathbf{V}_{0,h}^k \times Q_h^{k-1} : \\ \nu (\mathbf{u}_h, \mathbf{v}_h)_{\mathbf{H}_0^1(\Omega)} - (p_h, \operatorname{div} \mathbf{v}_h)_{L^2(\Omega)} = \nu (\mathbf{u}, \mathbf{v}_h)_{\mathbf{H}_0^1(\Omega)} - (z_{\mathbf{f}}, \operatorname{div} \mathbf{v}_h)_{L^2(\Omega)}, \\ (q_h, \operatorname{div} \mathbf{u}_h)_{L^2(\Omega)} + \nu^{-1} (p_h, q_h)_{L^2(\Omega)} = \nu^{-1} (z_{\mathbf{f}}, q_h)_{L^2(\Omega)}. \end{cases}$$

5.3. Convergence when $z_{\mathbf{f}}$ is known. Let $\Pi_{h,cg}$ be the $L^2(\Omega)$ -orthogonal projection operator from $L^2(\Omega)$ to $\mathbf{V}_{0,h}^k$ and $\Pi_{h,dg}$ be the $L^2(\Omega)$ -orthogonal projection operator from $L^2(\Omega)$ to $P_{disc}^{k-1}(\mathcal{T}_h)$. We have the

Proposition 7. *Let $(\mathbf{u}, p) \in \mathcal{X}$ be the solution to Problem (4.9) and $(\mathbf{u}_h, p_h) \in \mathcal{X}_h$ be the solution to Problem (5.3). We have the following error estimate:*

$$(5.5) \quad \|(\mathbf{u}_h - \mathbf{u}, p_h - \Pi_{h,dg} z_{\mathbf{f}})\|_{\mathcal{X},\nu} \leq (\sqrt{d} + 1) \|\mathbf{u} - \Pi_{h,cg} \mathbf{u}\|_{\mathbf{H}_0^1(\Omega)}.$$

Notice that the error estimate for the velocity is fully independent of the pressure. Hence, the (conforming) discretization of Problem (4.9) with $\mathbf{P}^k - P_{disc}^{k-1}$ is a so called *pressure robust method* for which the discrete velocity \mathbf{u}_h tends to \mathbf{u} independently of ν . The discrete pressure p_h tends to $\Pi_{h,dg} z_{\mathbf{f}}$ all the faster the smaller ν is. Interestingly, we remark that if $\mathbf{u} = 0$, then $\Pi_{h,cg} \mathbf{u} = 0$, so that $\mathbf{u}_h = 0$ and $p_h = \Pi_{h,dg} z_{\mathbf{f}}$, even for $k = 1$ (see Section 6.3). Let us now prove Proposition 7.

Proof. Setting $z_{\mathbf{f},h} = \Pi_{h,dg} z_{\mathbf{f}}$, we have: $(z_{\mathbf{f}}, \operatorname{div} \mathbf{v}_h)_{L^2(\Omega)} = (z_{\mathbf{f},h}, \operatorname{div} \mathbf{v}_h)_{L^2(\Omega)}$ and $(z_{\mathbf{f}}, q_h)_{L^2(\Omega)} = (z_{\mathbf{f},h}, q_h)_{L^2(\Omega)}$ for all $\mathbf{v}_h \in \mathbf{V}_{0,h}^k$, and all $q_h \in Q_h^{k-1}$. Summing both equations of Problem (5.4) and reshuffling terms, it comes:

$$(5.6) \quad \begin{cases} \text{Find } (\mathbf{u}_h, p_h) \in \mathbf{V}_{0,h}^k \times Q_h^{k-1} \text{ such that for all } (\mathbf{v}_h, q_h) \in \mathbf{V}_{0,h}^k \times Q_h^{k-1} : \\ \nu (\mathbf{u}_h - \mathbf{u}, \mathbf{v}_h)_{\mathbf{H}_0^1(\Omega)} + \nu^{-1} (p_h - z_{\mathbf{f},h}, q_h)_{L^2(\Omega)} \\ = (p_h - z_{\mathbf{f},h}, \operatorname{div} \mathbf{v}_h)_{L^2(\Omega)} - (q_h, \operatorname{div} \mathbf{u}_h)_{L^2(\Omega)}. \end{cases}$$

Choosing $\mathbf{v}_h = \mathbf{u}_h - \Pi_{h,cg} \mathbf{u} = (\mathbf{u}_h - \mathbf{u}) + (\mathbf{u} - \Pi_{h,cg} \mathbf{u})$ and $q_h = p_h - z_{\mathbf{f},h}$ in (5.6), and dividing by ν , we obtain:

$$\begin{aligned} & \| \mathbf{u}_h - \mathbf{u} \|_{\mathbf{H}_0^1(\Omega)}^2 + (\mathbf{u}_h - \mathbf{u}, \mathbf{u} - \Pi_{h,cg} \mathbf{u})_{\mathbf{H}_0^1(\Omega)} + \nu^{-2} \| p_h - z_{\mathbf{f},h} \|_{L^2(\Omega)}^2 \\ & = -\nu^{-1} (p_h - z_{\mathbf{f},h}, \operatorname{div} \Pi_{h,cg} \mathbf{u})_{L^2(\Omega)}. \end{aligned}$$

Hence, using Cauchy-Schwarz inequality, we get:

$$\|(\mathbf{u}_h - \mathbf{u}, p_h - z_{\mathbf{f},h})\|_{\mathcal{X},\nu}^2 \leq \| \mathbf{u}_h - \mathbf{u} \|_{\mathbf{H}_0^1(\Omega)} \| \mathbf{u} - \Pi_{h,cg} \mathbf{u} \|_{\mathbf{H}_0^1(\Omega)} + \nu^{-1} \| p_h - z_{\mathbf{f},h} \|_{L^2(\Omega)} \| \operatorname{div} \Pi_{h,cg} \mathbf{u} \|_{L^2(\Omega)}.$$

Since $\| \mathbf{u}_h - \mathbf{u} \|_{\mathbf{H}_0^1(\Omega)}$ and $\nu^{-1} \| p_h - z_{\mathbf{f},h} \|_{L^2(\Omega)}$ are each bounded by $\|(\mathbf{u}_h - \mathbf{u}, p_h - z_{\mathbf{f},h})\|_{\mathcal{X},\nu}$, and $\| \operatorname{div} \Pi_{h,cg} \mathbf{u} \|_{L^2(\Omega)} \leq \sqrt{d} \| \mathbf{u} - \Pi_{h,cg} \mathbf{u} \|_{\mathbf{H}_0^1(\Omega)}$, we have:

$$\begin{aligned} \|(\mathbf{u}_h - \mathbf{u}, p_h - z_{\mathbf{f},h})\|_{\mathcal{X},\nu} & \leq \| \mathbf{u} - \Pi_{h,cg} \mathbf{u} \|_{\mathbf{H}_0^1(\Omega)} + \| \operatorname{div} \Pi_{h,cg} \mathbf{u} \|_{L^2(\Omega)}, \\ & \leq (\sqrt{d} + 1) \| \mathbf{u} - \Pi_{h,cg} \mathbf{u} \|_{\mathbf{H}_0^1(\Omega)}. \end{aligned}$$

□

5.4. Convergence when $z_{\mathbf{f}}$ is not known. If $z_{\mathbf{f}}$ is not known explicitly, let us assume that we have at hand an approximation $\tilde{z}_{\mathbf{f},h} \in Q_h^{k-1}$ and use it to solve the following approximation of Problem (4.9):

$$(5.7) \quad \begin{cases} \text{Find } (\tilde{\mathbf{u}}, \tilde{p}) \in \mathcal{X} \text{ such that for all } (\mathbf{v}, q) \in \mathcal{X} : \\ \nu (\tilde{\mathbf{u}}, \mathbf{v})_{\mathbf{H}_0^1(\Omega)} - (\tilde{p}, \operatorname{div} \mathbf{v})_{L^2(\Omega)} = \langle \mathbf{f}, \mathbf{v} \rangle_{\mathbf{H}_0^1(\Omega)}, \\ (q, \operatorname{div} \tilde{\mathbf{u}})_{L^2(\Omega)} + \nu^{-1} (\tilde{p}, q)_{L^2(\Omega)} = \nu^{-1} (\tilde{z}_{\mathbf{f},h}, q)_{L^2(\Omega)}. \end{cases}$$

Let us write again $\mathbf{f} = -\nu\Delta\mathbf{u} + \mathbf{grad} z_{\mathbf{f}}$, so that Problem (5.7) reads:

$$(5.8) \quad \begin{cases} \text{Find } (\tilde{\mathbf{u}}, \tilde{p}) \in \mathcal{X} \text{ such that for all } (\mathbf{v}, q) \in \mathcal{X} : \\ \nu(\tilde{\mathbf{u}} - \mathbf{u}, \mathbf{v})_{\mathbf{H}_0^1(\Omega)} - (\tilde{p} - z_{\mathbf{f}}, \operatorname{div} \mathbf{v})_{L^2(\Omega)} = 0, \\ (q, \operatorname{div} \tilde{\mathbf{u}})_{L^2(\Omega)} + \nu^{-1}(\tilde{p} - \tilde{z}_{\mathbf{f},h}, q)_{L^2(\Omega)} = 0. \end{cases}$$

Proposition 8. *Let $(\mathbf{u}, p) \in \mathcal{X}$ be the solution to Problem (4.9) and $(\tilde{\mathbf{u}}, \tilde{p}) \in \mathcal{X}$ be the solution to Problem (5.7). We have the following estimates:*

$$(5.9) \quad \|\tilde{p} - z_{\mathbf{f}}\|_{L^2(\Omega)} \leq \|z_{\mathbf{f}} - \tilde{z}_{\mathbf{f},h}\|_{L^2(\Omega)} \quad \text{and} \quad \|\tilde{\mathbf{u}} - \mathbf{u}\|_{\mathbf{H}_0^1(\Omega)} \leq \nu^{-1} \|z_{\mathbf{f}} - \tilde{z}_{\mathbf{f},h}\|_{L^2(\Omega)}.$$

Proof. Choosing $\mathbf{v} = \tilde{\mathbf{u}} - \mathbf{u}$ and $q = \tilde{p} - z_{\mathbf{f}}$ in (5.8) and summing both equations, it comes:

$$\nu \|\tilde{\mathbf{u}} - \mathbf{u}\|_{\mathbf{H}_0^1(\Omega)}^2 + \nu^{-1} (\tilde{p} - \tilde{z}_{\mathbf{f},h}, \tilde{p} - z_{\mathbf{f}})_{L^2(\Omega)} = 0.$$

Writing $\tilde{p} - \tilde{z}_{\mathbf{f},h} = (\tilde{p} - z_{\mathbf{f}}) + (z_{\mathbf{f}} - \tilde{z}_{\mathbf{f},h})$, we obtain:

$$\|(\tilde{\mathbf{u}} - \mathbf{u}, \tilde{p} - z_{\mathbf{f}})\|_{\mathcal{X},\nu}^2 = -\nu^{-2} (z_{\mathbf{f}} - \tilde{z}_{\mathbf{f},h}, \tilde{p} - z_{\mathbf{f}})_{L^2(\Omega)} \leq \nu^{-2} \|z_{\mathbf{f}} - \tilde{z}_{\mathbf{f},h}\|_{L^2(\Omega)} \|\tilde{p} - z_{\mathbf{f}}\|_{L^2(\Omega)}.$$

We obtain successively estimates (5.9). \square

The discretization of Problem (5.7) with $\mathbf{P}^k - P_{disc}^{k-1}$ finite element reads:

$$(5.10) \quad \begin{cases} \text{Find } (\tilde{\mathbf{u}}_h, \tilde{p}_h) \in \mathbf{V}_{0,h}^k \times Q_h^{k-1} \text{ such that for all } (\tilde{\mathbf{v}}_h, \tilde{q}_h) \in \mathbf{V}_{0,h}^k \times Q_h^{k-1} : \\ \nu(\tilde{\mathbf{u}}_h, \mathbf{v}_h)_{\mathbf{H}_0^1(\Omega)} - (\tilde{p}_h, \operatorname{div} \mathbf{v}_h)_{L^2(\Omega)} = \langle \mathbf{f}, \mathbf{v}_h \rangle_{\mathbf{H}_0^1(\Omega)}, \\ (q_h, \operatorname{div} \tilde{\mathbf{u}}_h)_{L^2(\Omega)} + \nu^{-1}(\tilde{p}_h, q_h)_{L^2(\Omega)} = \nu^{-1}(\tilde{z}_{\mathbf{f},h}, q_h)_{L^2(\Omega)}. \end{cases}$$

Theorem 5. *Let $(\mathbf{u}, p) \in \mathcal{X}$ be the solution to Problem (4.9) and $(\tilde{\mathbf{u}}_h, \tilde{p}_h) \in \mathcal{X}$ be the solution to Problem (5.10). We have the following error estimate:*

$$(5.11) \quad \|(\tilde{\mathbf{u}}_h - \mathbf{u}, \tilde{p}_h - \Pi_{h,dg} z_{\mathbf{f}})\|_{\mathcal{X},\nu} \leq (\sqrt{d}+1) \|\mathbf{u} - \Pi_{h,cg} \mathbf{u}\|_{\mathbf{H}_0^1(\Omega)} + \nu^{-1} \|\Pi_{h,dg} z_{\mathbf{f}} - \tilde{z}_{\mathbf{f},h}\|_{L^2(\Omega)}.$$

Suppose that $\mathbf{u} = 0$. Then $\Pi_{h,cg} \mathbf{u} = 0$ and we obtain the estimate below:

$$(5.12) \quad \|(\tilde{\mathbf{u}}_h, \tilde{p}_h - \Pi_{h,dg} z_{\mathbf{f}})\|_{\mathcal{X},\nu} \leq \nu^{-1} \|\Pi_{h,dg} z_{\mathbf{f}} - \tilde{z}_{\mathbf{f},h}\|_{L^2(\Omega)}.$$

In particular, if $\tilde{z}_{\mathbf{f},h}$ is a convergent approximation of $\Pi_{h,dg} z_{\mathbf{f}}$, the solution $(\tilde{\mathbf{u}}_h, \tilde{p}_h)$ converges to $(\mathbf{u}, \Pi_{h,dg} z_{\mathbf{f}})$. Interestingly, the above with $k = 1$ corresponds to the $\mathbf{P}^1 - P^0$ finite element pair, which is known to be unstable for the discretization of the usual variational formulation (3.4) of the Stokes problem. Let us prove Theorem 5.

Proof. Setting $z_{\mathbf{f},h} = \Pi_{h,dg} z_{\mathbf{f}}$, we have: $\langle \mathbf{f}, \mathbf{v}_h \rangle_{\mathbf{H}_0^1(\Omega)} = \nu(\mathbf{u}, \mathbf{v}_h)_{\mathbf{H}_0^1(\Omega)} - (z_{\mathbf{f},h}, \operatorname{div} \mathbf{v}_h)_{L^2(\Omega)}$ for all $\mathbf{v}_h \in \mathbf{V}_{0,h}^k$. Hence, Problem (5.10) can be written as:

$$(5.13) \quad \begin{cases} \text{Find } (\tilde{\mathbf{u}}_h, \tilde{p}_h) \in \mathbf{V}_{0,h}^k \times Q_h^{k-1} \text{ such that for all } (\tilde{\mathbf{v}}_h, \tilde{q}_h) \in \mathbf{V}_{0,h}^k \times Q_h^{k-1} : \\ \nu(\tilde{\mathbf{u}}_h - \mathbf{u}, \mathbf{v}_h)_{\mathbf{H}_0^1(\Omega)} - (\tilde{p}_h - z_{\mathbf{f},h}, \operatorname{div} \mathbf{v}_h)_{L^2(\Omega)} = 0, \\ (q_h, \operatorname{div} \tilde{\mathbf{u}}_h)_{L^2(\Omega)} + \nu^{-1}(\tilde{p}_h - \tilde{z}_{\mathbf{f},h}, q_h)_{L^2(\Omega)} = 0. \end{cases}$$

Choosing $(\mathbf{v}_h, q_h) = (\tilde{\mathbf{u}}_h - \Pi_{h,cg} \mathbf{u}, \tilde{p}_h - z_{\mathbf{f},h})$ in Problem (5.13), we have:

$$\begin{cases} \nu(\tilde{\mathbf{u}}_h - \mathbf{u}, \tilde{\mathbf{u}}_h - \Pi_{h,cg} \mathbf{u})_{\mathbf{H}_0^1(\Omega)} - (\tilde{p}_h - z_{\mathbf{f},h}, \operatorname{div}(\tilde{\mathbf{u}}_h - \Pi_{h,cg} \mathbf{u}))_{L^2(\Omega)} = 0, \\ (\tilde{p}_h - z_{\mathbf{f},h}, \operatorname{div} \tilde{\mathbf{u}}_h)_{L^2(\Omega)} + \nu^{-1}(\tilde{p}_h - \tilde{z}_{\mathbf{f},h}, \tilde{p}_h - z_{\mathbf{f},h})_{L^2(\Omega)} = 0. \end{cases}$$

Summing both equations, it now comes:

$$\begin{aligned} \nu(\tilde{\mathbf{u}}_h - \mathbf{u}, \tilde{\mathbf{u}}_h - \Pi_{h,cg} \mathbf{u})_{\mathbf{H}_0^1(\Omega)} + \nu^{-1}(\tilde{p}_h - \tilde{z}_{\mathbf{f},h}, \tilde{p}_h - z_{\mathbf{f},h})_{L^2(\Omega)} \\ + (\tilde{p}_h - z_{\mathbf{f},h}, \operatorname{div} \Pi_{h,cg} \mathbf{u})_{L^2(\Omega)} = 0. \end{aligned}$$

Noticing that $\tilde{\mathbf{u}}_h - \Pi_{h,cg} \mathbf{u} = (\tilde{\mathbf{u}}_h - \mathbf{u}) + (\mathbf{u} - \Pi_{h,cg} \mathbf{u})$ and $\tilde{p}_h - \tilde{z}_{\mathbf{f},h} = (\tilde{p}_h - z_{\mathbf{f},h}) + (z_{\mathbf{f},h} - \tilde{z}_{\mathbf{f},h})$, dividing by ν , we get:

$$\begin{aligned} & \|(\tilde{\mathbf{u}}_h - \mathbf{u}, \tilde{p}_h - z_{\mathbf{f},h})\|_{\mathcal{X},\nu}^2 + (\tilde{\mathbf{u}}_h - \mathbf{u}, \mathbf{u} - \Pi_{h,cg} \mathbf{u})_{\mathbf{H}_0^1(\Omega)} \\ & + \nu^{-2} (z_{\mathbf{f},h} - \tilde{z}_{\mathbf{f},h}, \tilde{p}_h - z_{\mathbf{f},h})_{L^2(\Omega)} + \nu^{-1} (\tilde{p}_h - z_{\mathbf{f},h}, \operatorname{div} \Pi_{h,cg} \mathbf{u})_{L^2(\Omega)} = 0. \end{aligned}$$

Using Cauchy-Schwarz, we deduce that:

$$\begin{aligned} & \|(\tilde{\mathbf{u}}_h - \mathbf{u}, \tilde{p}_h - z_{\mathbf{f},h})\|_{\mathcal{X},\nu}^2 \leq \| \tilde{\mathbf{u}}_h - \mathbf{u} \|_{\mathbf{H}_0^1(\Omega)} \| \mathbf{u} - \Pi_{h,cg} \mathbf{u} \|_{\mathbf{H}_0^1(\Omega)} \\ & + \nu^{-1} \| \tilde{p}_h - z_{\mathbf{f},h} \|_{L^2(\Omega)} \left(\nu^{-1} \| z_{\mathbf{f},h} - \tilde{z}_{\mathbf{f},h} \|_{L^2(\Omega)} + \| \operatorname{div} \Pi_{h,cg} \mathbf{u} \|_{L^2(\Omega)} \right). \end{aligned}$$

Since $\| \tilde{\mathbf{u}}_h - \mathbf{u} \|_{\mathbf{H}_0^1(\Omega)}$ and $\nu^{-1} \| \tilde{p}_h - z_{\mathbf{f},h} \|_{L^2(\Omega)}$ are both bounded by $\|(\tilde{\mathbf{u}}_h - \mathbf{u}, \tilde{p}_h - z_{\mathbf{f},h})\|_{\mathcal{X},\nu}$, and $\| \operatorname{div} \Pi_{h,cg} \mathbf{u} \|_{L^2(\Omega)} \leq \sqrt{d} \| \mathbf{u} - \Pi_{h,cg} \mathbf{u} \|_{\mathbf{H}_0^1(\Omega)}$, we obtain the estimates (5.11) and (5.12). \square

6. NUMERICAL RESULTS

We propose some numerical experiments, depending on whether or not $z_{\mathbf{f}}$ is known explicitly. In the latter case, we first compute some approximation $\tilde{z}_{\mathbf{f},h}$. In principle, either a classical, conforming or nonconforming, discretization can be used to compute $\tilde{z}_{\mathbf{f},h}$. The numerical results are obtained on a github platform, implemented in Octave language (see [29] for order 1 and 2 nonconforming finite element methods).

6.1. Resolution algorithm. Consider the discretization of the classical variational formulation (3.4). Let $\mathbf{V}_{0,h}$ be the discrete velocity space, and Q_h be the discrete pressure space. Let $(\psi_i)_{i=1}^{N_u}$ be a basis of $\mathbf{V}_{0,h}$, and $(\phi_i)_{i=1}^{N_p}$ be a basis of Q_h . We set: $\underline{U} := (\underline{U}_i)_{i=1}^{N_u}$ where $\mathbf{u}_h := \sum_{i=1}^{N_u} \underline{U}_i \psi_i$, $\underline{P} := (\underline{P}_i)_{i=1}^{N_p}$ where $p_h := \sum_{i=1}^{N_p} \underline{P}_i \phi_i$, and $\underline{F}_u := (\underline{F}_{u,i})_{i=1}^{N_u}$. Suppose that $\mathbf{V}_{0,h} \subset \mathbf{H}_0^1(\Omega)$. Then $\underline{F}_{u,i} = \langle \mathbf{f}, \psi_i \rangle_{\mathbf{H}_0^1(\Omega)}$. Suppose that $\mathbf{V}_{0,h} \not\subset \mathbf{H}_0^1(\Omega)$, as it is the case using nonconforming Crouzeix-Raviart finite elements [13]. Let $\ell_{\mathbf{f}} \in \mathcal{L}(\mathbf{V}_{0,h}, \mathbb{R})$ be such that $\forall \mathbf{v}_h \in \mathbf{V}_{0,h}$, $\ell_{\mathbf{f}}(\mathbf{v}_h) = \langle \mathbf{f}, \mathbf{v}_h \rangle_{L^2(\Omega)}$ if $\mathbf{f} \in \mathbf{L}^2(\Omega)$, $\ell_{\mathbf{f}}(\mathbf{v}_h) = \langle \mathbf{f}, \mathcal{I}_h(\mathbf{v}_h) \rangle_{\mathbf{H}_0^1(\Omega)}$ if $\mathbf{f} \notin \mathbf{L}^2(\Omega)$, where $\mathcal{I}_h : \mathbf{V}_{0,h} \rightarrow \mathbf{V}_{0,h}^k$ is for instance an averaging operator [30, §22.4.1]. Then $\underline{F}_{u,i} = \ell_{\mathbf{f}}(\psi_i)$. Let $\mathbb{A} \in \mathbb{R}^{N_u} \times \mathbb{R}^{N_u}$ be the velocity stiffness matrix, $\mathbb{B} \in \mathbb{R}^{N_p} \times \mathbb{R}^{N_u}$ be the velocity-pressure coupling matrix and $\mathbb{M} \in \mathbb{R}^{N_p} \times \mathbb{R}^{N_p}$ be the pressure mass matrix.

The linear system to be solved is

$$(6.1) \quad \begin{cases} \text{Find } (\underline{U}, \underline{P}) \in \mathbb{R}^{N_u} \times \mathbb{R}^{N_p} \text{ such that:} \\ \nu \mathbb{A} \underline{U} - \mathbb{B}^T \underline{P} = \underline{F}_u \\ \mathbb{B} \underline{U} = 0 \end{cases}.$$

Let us set $\mathbb{K} = \mathbb{B} \mathbb{A}^{-1} \mathbb{B}^T \in \mathbb{R}^{N_p} \times \mathbb{R}^{N_p}$. The matrix $\mathbb{K} \in \mathbb{R}^{N_p} \times \mathbb{R}^{N_p}$ is a symmetric matrix, furthermore it is positive definite as soon as the kernel of \mathbb{B}^T is reduced to $\{0\}$. When it is the case, the linear system (6.1) can be solved with the help of the algorithm (6.3) below (with $\underline{F}_p = 0$).

Consider next the $\mathbf{P}^k - P_{disc}^{k-1}$ conforming discretization of the variational formulation (5.3) or (5.10). Let $(\psi_i)_{i=1}^{N_u}$ be the Lagrange basis of $\mathbf{V}_{0,h}^k$ and $(\phi_i)_{i=1}^{N_p}$ be the basis of Q_h^{k-1} . We set: $\underline{U} := (\underline{U}_i)_{i=1}^{N_u}$ where $\mathbf{u}_h := \sum_{i=1}^{N_u} \underline{U}_i \psi_i$ and $\underline{P} := (\underline{P}_i)_{i=1}^{N_p}$ where $p_h := \sum_{i=1}^{N_p} \underline{P}_i \phi_i$. We set $\underline{F}_u := (\underline{F}_{u,i})_{i=1}^{N_u}$ where $\underline{F}_{u,i} = \langle \mathbf{f}, \psi_i \rangle_{\mathbf{H}_0^1(\Omega)}$ and $\underline{F}_p := (\underline{F}_{p,i})_{i=1}^{N_p}$ where $\underline{F}_{p,i} = (z_{\mathbf{f}}, \phi_i)_{L^2(\Omega)}$, cf. (5.3), or $\underline{F}_{p,i} = (\tilde{z}_{\mathbf{f},h}, \phi_i)_{L^2(\Omega)}$,

where the discrete pressure $\tilde{z}_{\mathbf{f},h}$ is an approximation of $z_{\mathbf{f}}$, cf. (5.10). The linear system to be solved is

$$(6.2) \quad \begin{cases} \text{Find } (\underline{U}, \underline{P}) \in \mathbb{R}^{N_u} \times \mathbb{R}^{N_p} \text{ such that:} \\ \nu \mathbb{A} \underline{U} - \mathbb{B}^T \underline{P} = \underline{F}_u \\ \mathbb{B} \underline{U} + \nu^{-1} \mathbb{M} \underline{P} = \nu^{-1} \underline{F}_p \end{cases}.$$

In that case, we set $\mathbb{K} = \mathbb{B} \mathbb{A}^{-1} \mathbb{B}^T + \mathbb{M} \in \mathbb{R}^{N_p} \times \mathbb{R}^{N_p}$, which is automatically a symmetric positive definite matrix.

To solve the coupled velocity-pressure problem (6.1) or (6.2), one relies usually on the three + one steps below (the fourth step being straightforward):

$$(6.3) \quad \begin{array}{ll} \text{Prediction:} & \text{Solve in } \underline{U}_\star \text{ such that } \nu \mathbb{A} \underline{U}_\star = \underline{F}_u. \\ \text{Pressure solver:} & \text{Solve in } \underline{P} \text{ such that } \mathbb{K} \underline{P} = \underline{F}_p - \nu \mathbb{B} \underline{U}_\star. \\ \text{Correction:} & \text{Solve in } \delta \underline{U} \text{ such that } \nu \mathbb{A} \delta \underline{U} = \mathbb{B}^T \underline{P}. \\ \text{Update:} & \underline{U} = \delta \underline{U} + \underline{U}_\star. \end{array}$$

Indeed, one can check easily that the above computed solution $(\underline{U}, \underline{P})$ solves (6.1) (resp. (6.2)). The pressure solver with matrix \mathbb{K} is based on the Uzawa algorithm, which is the conjugate gradient algorithm in the context of the Stokes problem. It can be preconditioned by the inverse of the mass matrix associated to the discrete pressure \mathbb{M} (see e.g. [31, Lemma 5.9]). Thanks to the uniform discrete inf-sup condition, the number of iterations of the conjugate gradient algorithm is independent of the meshsize.

To solve (6.2), matrices \mathbb{M} and \mathbb{B} are kept with all the P_{disc}^{k-1} degrees of freedom for the discrete pressure. To take into account the zero mean value constraint, at each iteration of the preconditioned conjugate gradient algorithm, the discrete pressure is first computed in $L^2(\Omega)$, then orthogonally projected in $L_{zmv}^2(\Omega)$. We use the Cholesky factorization (computed once and for all) to solve linear systems with matrix \mathbb{A} . In addition, for $k = 2$, one can use the lumped mass matrix (for $k = 1$, the mass matrix is diagonal). In the numerical results proposed below, we use the same strategy to solve (6.1) with nonconforming Crouzeix-Raviart finite elements [13].

Remark 1. *We recall that solving the linear system (6.1) via the solver (6.3) is not so straightforward, even with $\nu = 1$. At first glance, solving the linear system (6.2) via the solver (6.3) may seem also quite involved. On the other hand, the preconditioned matrix $\mathbb{M}^{-1/2} \mathbb{K} \mathbb{M}^{-1/2}$ is better conditioned in the latter case thanks to the addition of \mathbb{M} in the definition of \mathbb{K} .*

6.2. Settings. We consider Problem (3.1) with $\Omega = (0, 1)^2$. Let (\mathbf{u}, p) be the exact solution, and (\mathbf{u}_h, p_h) be the numerical solution. On Figures 1 to 7, and in Tables 2 to 6 we give the following names to our numerical methods:

- CR-method: computations are made with the nonconforming Crouzeix-Raviart $\mathbf{P}_{nc}^1 - P^0$ formulation [13, Example 4], which is not a pressure robust method. We call p_{nc} the resulting discrete pressure.
- EP-method: computations are made with the coercive $\mathbf{P}^1 - P^0$ formulation (5.3), knowing the exact pressure (EP) $z_{\mathbf{f}}$ (i.e. we solve Problem (5.3)).
- TS-method: computations are made in two steps (TS). In a first step, we approximate the pressure by the CR-method. Then, in a post processing step, we use this numerical pressure as the source term in the EP-method

(i.e. we solve Problem (5.10) with $\tilde{z}_{\mathbf{f},h} = p_{nc}$). Possibly, we iterate eight times the second step, updating $\tilde{z}_{\mathbf{f},h}$ at each new iteration.

Let N_T be the number of triangles. For the velocity, the number of unknowns is of order $N_u \approx 3N_T$ for the CR-method and $N_u \approx N_T$ for the EP-method. For the pressure, the number of unknowns is $N_p = N_T$ for both methods. As a consequence, there are roughly twice as many unknowns for the CR-method than there are for the EP-method. We report in Table 1 the number of unknowns ”# dof” for the numerical tests. In addition, we observe that, with the same stopping criterion, around 30 (resp. 15) iterations of the preconditioned conjugate gradient algorithm are needed to solve the pressure solver of algorithm (6.3) with the CR-method (resp. with the EP-method): this is consistent with Remark 1.

h	# dof CR	# dof EP	# dof CR	# dof EP
$1.00 e - 1$	1 048	566	2 184	1 114
$5.00 e - 2$	4 376	2 270	8 064	4 074
$2.50 e - 2$	17 368	8 846	30 464	15 314
$1.25 e - 2$	67 816	34 230	117 664	58 994
$6.25 e - 3$	272 624	136 954	464 448	232 866

TABLE 1. Number of unknowns: first two test cases (left), last test case (right).

We propose three numerical examples based on manufactured solutions. We first plot the results as error curves for both the velocity and the pressure as a function of the meshsize, and we give the numerically observed average convergence rates. Second, we report the elapsed CPU times for the CR-method and the TS-method. In the Tables, column ”overhead” indicates the ratio between the cost of the second (post processing) step for the TS-method and the cost of the first step (CR-method). Finally, we plot the errors of the two methods as a function of the elapsed CPU times.

6.3. Regular manufactured solutions. We postulate that for the EP-method and the TS-method, $\|\mathbf{u} - \mathbf{u}_h\|_{\mathbf{L}^2(\Omega)} \leq C_0 \|(\mathbf{u}, p)\|_{\mathcal{X},\nu} h^2$, where C_0 is independent of the meshsize. The error estimates for the CR-method are given by [13, Theorems 3, 4, 6]. Notice that the norm $\|(\cdot, \cdot)\|_{\mathcal{X},\nu}$ depends on the viscosity ν (3.5) and that the error estimates on the pressure and the velocity are linked. We check the convergence rates and the viscosity dependency of the error estimates. The first test enters the framework of §5.3, see the estimate (5.5).

- **Test case with a vanishing velocity: Figure 1.**

We consider Problem (3.1) with $\mathbf{f} = \mathbf{grad} p$, where: $(\mathbf{u}, p) = (0, x^3 + y^3 - 1/2)$. The number of unknowns are reported on Table 1 (left). Figure 1 shows the discrete error values $\varepsilon_0'(\mathbf{u}_h) := \nu \|\mathbf{u}_h\|_{\mathbf{L}^2(\Omega)} / \|p\|_{L^2(\Omega)}$ (left) and $\varepsilon_0(p_h) := \|p - p_h\|_{L^2(\Omega)} / \|p\|_{L^2(\Omega)}$ (right) plotted against the meshsize. We note that the discrete errors for the pressure are independent of $\nu > 0$. As a matter of fact, since the continuous velocity vanishes, i.e. $\mathbf{u} = 0$, the linear system corresponding to the pressure solver step in the algorithm (6.3) does not depend on ν . As expected in (5.5), the EP-method returns $\varepsilon_0'(\mathbf{u}_h) = \mathcal{O}(10^{-15})$

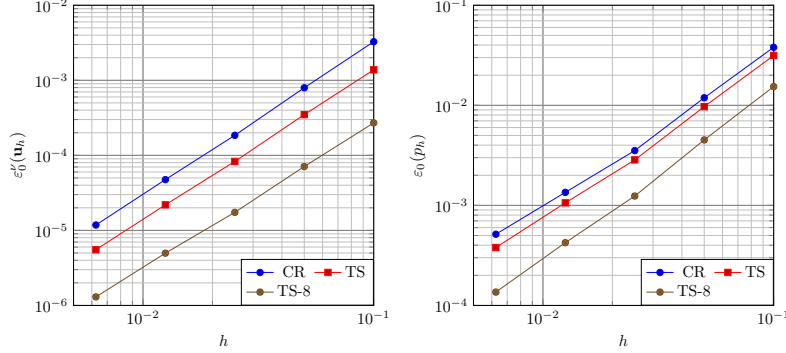


FIGURE 1. Vanishing velocity. Plots of $\varepsilon_0'(\mathbf{u}_h)$ and $\varepsilon_0(p_h)$ for $\nu = 1$ or $\nu = 10^{-6}$.

and $\varepsilon_0(p_h) = \mathcal{O}(10^{-13})$, so the errors are not reported on Figure 1. For the CR-method, the average convergence rate for the velocity, $\tau_{\mathbf{u}}$ is 2.03, while the average convergence rate for the pressure, τ_p is 1.55, which is better than expected, possibly because the source term is a polynomial of degree 2 which is numerically exactly integrated. For the TS-method, "TS" plots represent the errors after a single iteration of the second step and "TS-8" plots represent the errors after iterating the second step eight times, updating $\tilde{z}_{f,h}$ at each new iteration. Both post-processings improve the initial computation of the velocity. Using eight iterations allows to improve the accuracy of the discrete pressure. For the TS-method with a single iteration (resp. eight iterations), the average convergence rate for the velocity, $\tau_{\mathbf{u}}$ is 1.99 (resp. 1.93), while the average convergence rate for the pressure, τ_p is 1.71 (resp. 1.71). Figure 2 shows the discrete error values $\varepsilon_0'(\mathbf{u}_h)$ (left) and $\varepsilon_0(p_h)$ (right) plotted against the CPU time.

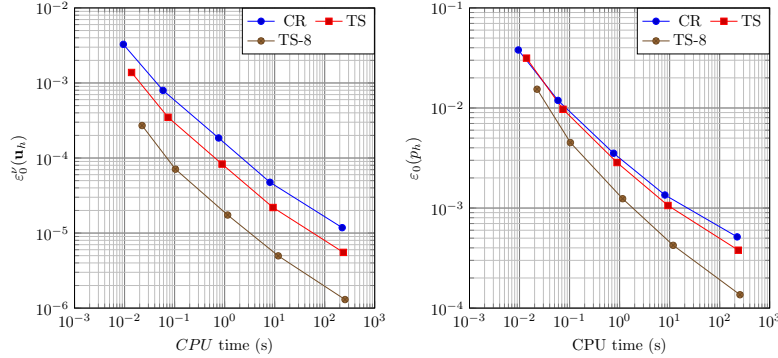


FIGURE 2. Vanishing velocity. Plots of $\varepsilon_0'(\mathbf{u}_h)$ and $\varepsilon_0(p_h)$ for $\nu = 1$ or $\nu = 10^{-6}$ against CPU time.

Table 2 below shows the CPU times for the CR-method and the TS-method with either one, or eight, iterations. By design, the TS-method which includes the CR-method as its first step requires more CPU time. However, we notice that the CPU time of the second (post processing) step, the overhead, is only a small fraction

h	CPU CR	CPU TS	overhead	CPU TS-8	overhead
$1.00 e - 1$	$9.46 e - 3$	$1.38 e - 2$	46 %	$2.24 e - 2$	136 %
$5.00 e - 2$	$5.88 e - 2$	$7.40 e - 2$	26 %	$1.04 e - 1$	77 %
$2.50 e - 2$	$7.59 e - 1$	$8.89 e - 1$	17 %	$1.15 e + 0$	52 %
$1.25 e - 2$	$8.06 e + 0$	$9.28 e + 0$	15 %	$1.18 e + 1$	47 %
$6.25 e - 3$	$2.24 e + 2$	$2.36 e + 2$	5 %	$2.55 e + 2$	14 %

TABLE 2. CPU time (s), vanishing velocity for $\nu = 10^{-6}$.

of the first step, and also that it decreases dramatically as the meshsize decreases. This can be explained by the fact that on the one hand, there are fewer unknowns and, on the other hand, the pressure solver converges faster (cf. Remark 1). For the TS-method, it seems worth doing eight iterations, especially when the meshsize is small.

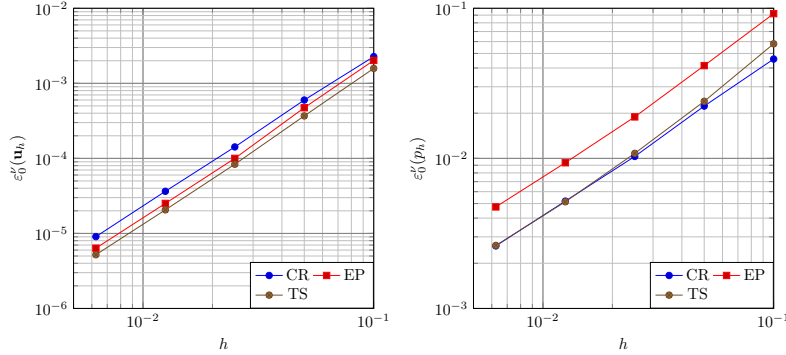
- **Test case with a sinusoidal solution: Figures 3-5**

We consider Problem (3.1) with $\mathbf{f} = -\nu \Delta \mathbf{u} + \mathbf{grad} p$, where:

$$\mathbf{u} = \begin{pmatrix} (1 - \cos(2\pi x)) \sin(2\pi y) \\ (\cos(2\pi y) - 1) \sin(2\pi x) \end{pmatrix} \text{ and } p = \sin(2\pi x) \sin(2\pi y).$$

The number of unknowns are reported on Table 1 (left). The discrete errors values are $\varepsilon_0^\nu(\mathbf{u}_h) := \|\mathbf{u} - \mathbf{u}_h\|_{L^2(\Omega)} / \|(\mathbf{u}, p)\|_{\mathcal{X}, \nu}$ for the velocity and $\varepsilon_0^\nu(p_h) := \nu^{-1} \|p - p_h\|_{L^2(\Omega)} / \|(\mathbf{u}, p)\|_{\mathcal{X}, \nu}$ for the pressure.

Figure 3 shows $\varepsilon_0^\nu(\mathbf{u}_h)$ (left) and $\varepsilon_0^\nu(p_h)$ (right) plotted against the meshsize, for $\nu = 1$. In that case, for the TS-method, there is no need doing eight iterations, so we give numerical results for computations with a single iteration only.

FIGURE 3. Sinusoidal velocity, $\nu = 1$. Plots of $\varepsilon_0^\nu(\mathbf{u}_h)$ and $\varepsilon_0^\nu(p_h)$.

The TS-method and the EP-method give similar velocity errors. The CR-method and the TS-method give similar pressure errors. For a given meshsize h , the velocity error is smaller for the EP-method and the TS-method than for the CR-method; and the pressure error is smaller for the CR-method than for the EP-method, but it is obtained at a higher cost. Notice that the TS-method reduces the velocity error without worsening the pressure error.

Figure 4 shows $\varepsilon_0^\nu(\mathbf{u}_h)$ (left) and $\varepsilon_0^\nu(p_h)$ (right) plotted against the meshsize, now

for $\nu = 10^{-6}$. For the TS-method, "TS" plots represent the errors after a single iteration of the second step and "TS-8" plots represent the errors after iterating the second step eight times, updating $\tilde{z}_{f,h}$ at each new iteration. Both post-processings improve the initial computation. Even with eight iterations, the overhead cost remains affordable, especially when the meshsize is small.

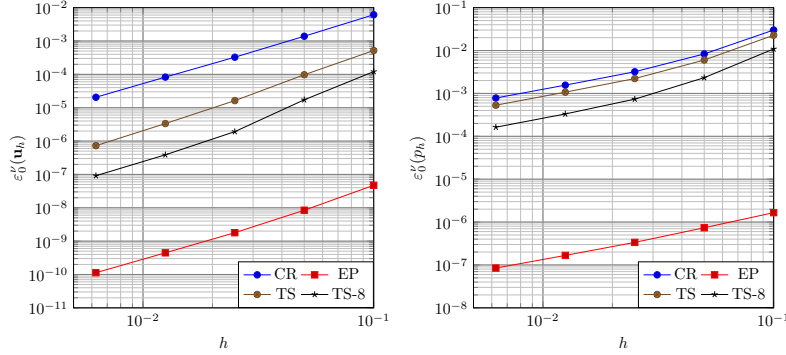


FIGURE 4. Sinusoidal velocity, $\nu = 10^{-6}$. Plots of $\varepsilon_0^\nu(\mathbf{u}_h)$ and $\varepsilon_0^\nu(p_h)$.

The EP-method gives much smaller velocity and pressure errors than the CR-method since it is a pressure robust method. For a given meshsize h , we note that the TS-method allows to reduce the velocity error by a factor larger than 10. The pressure error of the TS-method using one iteration is similar to that of the CR-method, while it is improved using eight iterations.

Table 3 shows the average convergence rates for the velocity, $\tau_{\mathbf{u}}$ and the pressure, τ_p .

ν	τ	CR	EP	TS	TS-8
1	$\tau_{\mathbf{u}}$	1.98	2.08	2.06	—
	τ_p	1.03	1.07	1.12	—
10^{-6}	$\tau_{\mathbf{u}}$	2.06	2.18	2.37	2.59
	τ_p	1.32	1.07	1.36	1.52

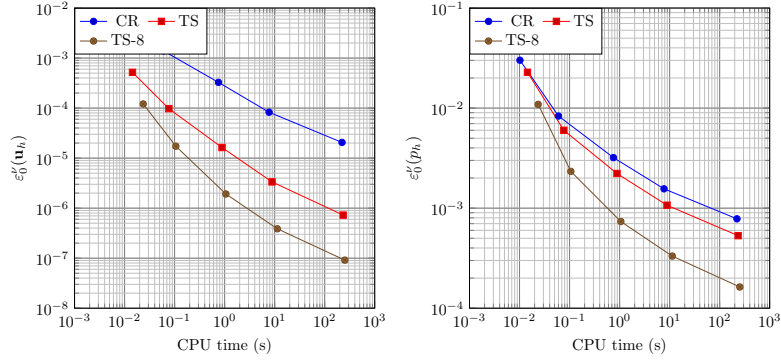
TABLE 3. Average convergence rates, sinusoidal velocity.

In the case $\nu = 1$, the average convergence rates are as expected. In the case $\nu = 10^{-6}$, the average convergence rate for the velocity, $\tau_{\mathbf{u}}$, is better than expected for the EP-method and the TS-method, and the average convergence rate for the pressure, τ_p , is better than expected for the TS-method, probably because the asymptotic convergence regime has not been reached.

Table 4 below shows the CPU times for the CR-method and the TS-method with either one, or eight, iterations. As we have used the same meshes, the computation times are similar to those in Table 2, showing once again that the overhead cost decreases dramatically as the mesh size decreases.

Figure 5 shows $\varepsilon_0^\nu(\mathbf{u}_h)$ (right) and $\varepsilon_0^\nu(p_h)$ (left) plotted against the CPU time for the CR-method and the TS-method with a single iteration ("TS" plot) or eight iterations ("TS-8" plot).

h	CPU CR	CPU TS	overhead	CPU TS-8	overhead
$1.00 e - 1$	$1.02 e - 2$	$1.44 e - 2$	41 %	$2.36 e - 2$	131 %
$5.00 e - 2$	$6.01 e - 2$	$7.68 e - 2$	28 %	$1.06 e - 1$	76 %
$2.50 e - 2$	$7.54 e - 1$	$8.87 e - 1$	18 %	$1.16 e + 0$	54 %
$1.25 e - 2$	$7.73 e + 0$	$8.87 e + 0$	15 %	$1.13 e + 1$	46 %
$6.25 e - 3$	$2.22 e + 2$	$2.34 e + 2$	5 %	$2.53 e + 2$	14 %

TABLE 4. CPU time (s), sinusoidal velocity for $\nu = 10^{-6}$.FIGURE 5. Sinusoidal velocity, $\nu = 10^{-6}$. Plots of $\varepsilon_0^\nu(\mathbf{u}_h)$ and $\varepsilon_0^\nu(p_h)$ against CPU time.

To achieve $\varepsilon_0^\nu(\mathbf{u}_h) \lesssim 5 \times 10^{-5}$, the required CPU time is 1 s for the TS-method with one iteration and 0.1 s for the TS-method with eight iterations, to be compared with more than 200 s with the CR-method.

• Some observations

The coercive $\mathbf{P}^1 - P^0$ formulation (EP-method) gives *pressure robust* results, the obvious limitation being that it requires to know explicitly the potential of the gradient part of the source term. If it is not known, the two step method reduces the velocity error, compared with the calculation carried out using the Crouzeix-Raviart $\mathbf{P}_{nc}^1 - P^0$ formulation (CR-method). Moreover, using the second (post processing) step *iteratively* greatly improves the initial result. Finally, the reduction factor is greater the smaller ν is.

6.4. Low regularity manufactured solution. We now consider a low regularity solution. Let (ρ, θ) be the polar coordinates centered in $(0.5, 0.5)$. Let $\alpha = 0.45$. We set $\mathbf{f} = -\nu \Delta \mathbf{u} + \mathbf{grad} p$ where $(\mathbf{u}, p) = (\rho^\alpha \mathbf{e}_\theta, \rho - \int_\Omega \rho)$. Results are given for $\nu = 10^{-6}$. For the TS-method, we systematically iterate eight times the second step, updating $\tilde{\mathbf{z}}_{\mathbf{f}, h}$ at each new iteration. The number of unknowns are reported on Table 1 (right). We used a refined mesh around $(0.5, 0.5)$, where the solution is of low regularity. Figure 6 shows the discrete error values $\varepsilon_0^\nu(\mathbf{u}_h) := \|\mathbf{u} - \mathbf{u}_h\|_{\mathbf{L}^2(\Omega)} / \|(\mathbf{u}, p)\|_{\mathcal{X}, \nu}$ (left) and $\varepsilon_0^\nu(p_h) := \nu^{-1} \|p - p_h\|_{L^2(\Omega)} / \|(\mathbf{u}, p)\|_{\mathcal{X}, \nu}$ (right) plotted against the mesh-size.

We remark that EP-method shows far better results than the CR-method, and that the TS-method allows again to improve the approximation of the CR-method.

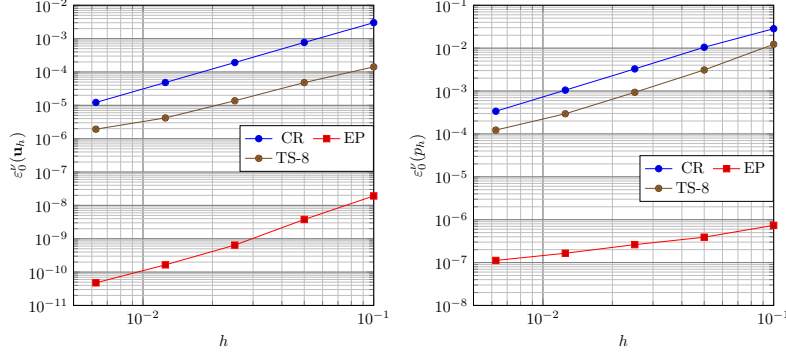
FIGURE 6. Low regularity velocity, $\nu = 10^{-6}$. Plots of $\varepsilon_0^\nu(\mathbf{u}_h)$ and $\varepsilon_0^\nu(p_h)$.

Table 5 shows the averaged convergence rates between the successive meshes.

τ	CR	EP	TS-8
$\tau_{\mathbf{u}}$	2.0	1.9	1.5
τ_p	1.6	0.6	1.5

TABLE 5. Convergence rates, low regularity velocity, $\nu = 10^{-6}$.

For the EP-method and the CR-method, we postulate that, asymptotically, $\tau_{\mathbf{u}} = 1 + \alpha$ and $\tau_p = \alpha$. In both cases, the obtained convergence rates are better than expected, which suggest that the asymptotic convergence regime is not reached. It seems that it will be reached faster for the EP-method, probably because it is pressure robust.

Table 6 below shows the CPU times for the CR-method and the TS-method with eight iterations. Again, the overhead cost decreases sharply with the meshsize.

h	CPU CR	CPU TS-8	overhead
$1.00 e - 1$	$2.34 e - 2$	$5.88 e - 2$	123 %
$5.00 e - 2$	$2.42 e - 1$	$3.71 e - 1$	53 %
$2.50 e - 2$	$2.28 e + 0$	$3.46 e - 0$	52 %
$1.25 e - 2$	$2.43 e + 1$	$3.39 e + 1$	39 %
$6.25 e - 3$	$6.86 e + 2$	$7.74 e + 2$	12 %

TABLE 6. CPU time (s), low regularity velocity for $\nu = 10^{-6}$.

Figures 7 show the discrete error values $\varepsilon_0^\nu(\mathbf{u}_h)$ (left) and $\varepsilon_0^\nu(p_h)$ (right) against the CPU time for the CR-method and the TS-method with eight iterations.

To achieve $\varepsilon_0^\nu(\mathbf{u}_h) \lesssim 2 \times 10^{-5}$, the CPU time is in the order of 250 s with the CR-method, compared to roughly 2 s with the TS-method with eight iterations.

7. CONCLUSION

We proposed and analysed a new variational formulation of Stokes problem based on T -coercivity theory. This variational formulation is coercive, and can be discretized with the $\mathbf{P}^k - P_{disc}^{k-1}$ finite element for all $k \geq 1$. To solve the linear system

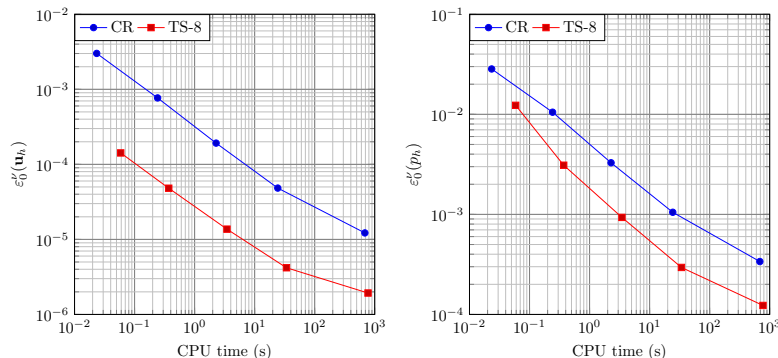


FIGURE 7. Low regularity velocity, $\nu = 10^{-6}$. Plots of $\varepsilon'_0(\mathbf{u}_h)$ and $\varepsilon'_0(p_h)$ against CPU time.

resulting from the discretization, we need to know the pressure, or at least some approximation of it, which in our numerical tests is the discrete pressure obtained using the classical non-conforming method with the Crouzeix-Raviart $\mathbf{P}_{nc}^1 - P^0$ finite element. This two step method improves the numerical results by notably reducing the errors obtained after the use of the classical method, especially when the viscosity is small. More significantly, the two step method consistently outperforms the classical method in terms of precision with respect to CPU time. Interestingly, this two step approach could be used in principle to solve the time-dependent Navier-Stokes equations with the help of the $\mathbf{P}^k - P_{disc}^{k-1}$ finite element, as soon as an initial discrete pressure computed with a stable finite element pair is available.

REFERENCES

- [1] L. Chesnel and P. Ciarlet Jr. T -coercivity and continuous Galerkin methods: application to transmission problems with sign changing coefficients. *Numer. Math.*, 124:1–29, 2013.
- [2] V. Girault and P.-A. Raviart. *Finite element methods for Navier-Stokes equations*. Springer-Verlag, 1986.
- [3] P. Ciarlet Jr. T -coercivity: Application to the discretization of Helmholtz-like problems. *Computers & Mathematics with Applications*, 64(1):22–24, 2012.
- [4] A. Ern and J.-L. Guermond. *Finite elements II*, volume 73 of *Texts in Applied Mathematics*. Springer, 2021.
- [5] E. Jamelot and P. Ciarlet Jr. Fast non-overlapping Schwarz domain decomposition methods for solving the neutron diffusion equation. *Journal of Computational Physics*, 241:445–463, 2013.
- [6] P. Ciarlet Jr., E. Jamelot, and F.D. Kpadonou. Domain decomposition methods for the diffusion equation with low-regularity solution. *Computers & Mathematics with Applications*, 74(10):2369–2384, 2017.
- [7] L. Giret. *Non-Conforming Domain Decomposition for the Multigroup Neutron SPN Equation*. PhD thesis, Université Paris-Saclay, 2018.
- [8] P. Ciarlet Jr. and E. Jamelot. Variational methods for solving numerically magnetostatic systems. *Advances in Computational Mathematics*, to appear.
- [9] M. Barré and P. Ciarlet Jr. The T -coercivity approach for mixed problems. *C. R. Acad. Sci. Paris, Ser. I.*, to appear.
- [10] A.-S. Bonnet-Ben Dhia and P. Ciarlet Jr. Variational methods for the analysis of noncoercive problems (in French), 2022. M.Sc. AMS Lecture Notes (Institut Polytechnique de Paris, France).
- [11] F. Boyer and P. Fabrie. *Mathematical tools for the study of the incompressible Navier-Stokes equations and related models*. Springer-Verlag, 2013.

- [12] C. Taylor and T. Hood. Numerical solution of the Navier-Stokes equations using the finite element technique. *Computers & Fluids*, 1:73–100, 1973.
- [13] M. Crouzeix and P.-A. Raviart. Conforming and nonconforming finite element methods for solving the stationary Stokes equations. *RAIRO, Sér. Anal. Numér.*, 7(3):33–75, 1973.
- [14] D. Boffi, F. Brezzi, and M. Fortin. *Mixed and hybrid finite element methods and applications*. Springer-Verlag, 2013.
- [15] E. Jamelot. Improved stability estimates for solving Stokes problem with Fortin-Soulie finite elements. Technical Report HAL, 2023.
- [16] C. Bernardi and G. Raugel. Méthodes d’éléments finis mixtes pour les equations de Stokes et de Navier-Stokes dans un polygone non convexe. *Calcolo*, 18:255–291, 1981.
- [17] D. N. Arnold, F. Brezzi, and M. Fortin. A stable finite element for the Stokes equations. *Calcolo*, 21:337–344, 1984.
- [18] G. R. Barrenechea and F. Valentin. An unusual stabilized finite element method for a generalized Stokes problem. *Numerische Mathematik*, 92:653–677, 2002.
- [19] N. Chaabane, V. Girault, B. Riviere, and T. Thompson. A stable enriched Galerkin element for the Stokes problem. *Applied Numerical Mathematics*, 132:1–21, 2018.
- [20] Y. Li and L. T. Zikatanov. New stabilized $P_1 \times P_0$ finite element methods for nearly inviscid and incompressible flows. *Computer Methods in Applied Mechanics and Engineering*, 393:114815, 2022.
- [21] P. B. Bochev, C. R. Dohrmann, and M. D. Gunzburger. Stabilization of low-order mixed finite elements for the Stokes equations. *SIAM Journal on Numerical Analysis*, 44(1):82–20, 2006.
- [22] G. R. Barrenechea and F. Valentin. Consistent Local Projection Stabilized Finite Element Methods. *SIAM Journal on Numerical Analysis*, 48(5):1801–1825, 2010.
- [23] T. Zhang and L. Tang. A stabilized finite volume method for Stokes equations using the lowest order $P_1 - P_0$ element pair. *Adv Comput Math*, 41:781–798, 2015.
- [24] A. Allendes, G. R. Barrenechea, and C. Naranjo. A divergence-free low-order stabilized finite element method for a generalized steady state Boussinesq problem. *Computer Methods in Applied Mechanics and Engineering*, 340:90–120, 2018.
- [25] M. Ainsworth, A. Allendes, G. R. Barrenechea, and R. Rankin. On the Adaptive Selection of the Parameter in Stabilized Finite Element Approximations. *SIAM Journal on Numerical Analysis*, 51(3):1585–1609, 2013.
- [26] L. R. Scott and M. Vogelius. Conforming finite element methods for incompressible and nearly incompressible continua. In *Lectures in Applied Mathematics, Part 2*, volume 22-2, pages 221–244. Amer. Math. Soc., 1985.
- [27] S. Zhang. A new family of stable mixed finite elements for the 3D Stokes equations. *Mathematics of Computation*, 74:543–554, 2005.
- [28] G. R. Barrenechea, E. Burman, E. Cáceres, and J. Guzmán. Continuous interior penalty stabilization for divergence-free finite element methods. *IMA Journal of Numerical Analysis*, 2023.
- [29] E. Jamelot. Stokes_NCFEM code. https://github.com/cea-trust-platform/Stokes_NCFEM, 2022.
- [30] A. Ern and J.-L. Guermond. *Finite elements I*, volume 72 of *Texts in Applied Mathematics*. Springer, 2021.
- [31] M. A. Olshanskii and E. E. Tyrtshnikov. *Iterative Methods for Linear Systems*. Society for Industrial and Applied Mathematics, Philadelphia, PA, 2014.